Spectra of acceptors in quantum dots: the effect of a magnetic field

1999 J. Phys.: Condens. Matter 11 1079

(http://iopscience.iop.org/0953-8984/11/4/015)

J. Phys.: Condens. Matter **11** (1999) 1079–1088. Printed in the UK PII: S0953-8984(99)96998-9

Spectra of acceptors in quantum dots: the effect of a magnetic field

M Pacheco†§ and Z Barticevic‡‖

† Departamento de Física, Universidad de Santiago de Chile, Casilla 307, Santiago, Chile
‡ Departamento de Física, Universidad Técnica F Santa María, Casilla 110-V, Valparaíso, Chile

Received 24 August 1998, in final form 27 October 1998

Abstract. We report calculations of the energy spectra of shallow-acceptor impurities in $GaAs/Ga_{1-x}Al_xAs$ quantum dots in the presence of external magnetic fields. We calculate the binding energies of the ground and excited acceptor states in the effective-mass approximation using a formalism based on a four-band model that includes the coupling of the spin to the magnetic field as well as the valence-band mixing. The potential of the acceptor is taken to be the screened Coulomb potential of a point charge, and we take into account the mismatch of the dielectric constant through the method of image charges. We present a complete analysis of the acceptor binding energies as a function of the lateral confinement of the quantum dot and as a function of the magnetic field strength. We also discuss the role of the mixing of heavy holes and light holes in determining the acceptor spectrum in the different regimes of confinement.

1. Introduction

Low-dimensional semiconductor structures have been the subject of many theoretical and experimental investigations during the last few years. New effects originating from the decreased dimensionality of these systems have been predicted theoretically and are the basis of potential applications to novel optical and electronic devices [1]. Recent advances in nano-fabrication techniques have made possible the realization of one-dimensional structures or quantum wires, and zero-dimensional structures, called quantum dots. These quantum nano-structures are fabricated starting from a quantum well structure, which is modified by lithographic and etching techniques to achieve the lateral confinement [2, 3]. The electronic and optical properties of these nanostructures are strongly modified with respect to those of the host materials due to the quantum confinement effects [4, 5].

The energy spectrum for residual, or intentionally introduced, impurities in low-dimensional systems is important both as a fundamental problem and also because of its relevance to the fabrication of electronic devices. Shallow-impurity-related properties of quantum wells, quantum wires, and quantum dots have been the subject of extensive research in the last few years. The physical properties of these quantum heterostructures can be artificially varied over a wide range, and a large spread of impurity binding energies can be obtained. Most of the calculations have shown that due to the higher degree of confinement in quantum dots the impurity binding energies are larger than those for impurities in quantum wells and quantum wires [6].

§ E-mail address: mpacheco@lauca.usach.cl.
‖ E-mail address: zbartice@fis.utfsm.cl.

0953-8984/99/041079+10$19.50

As for bulk semiconductors, the electronic energy spectra of low-dimensional systems are strongly affected by the presence of external fields. In the case of quantum wires and quantum dots, in the presence of a magnetic field, there is an interesting competition between the magnetic confinement and the geometrical confinement, which greatly influences their electronic and optical properties. Shallow-impurity states in quantum wells in the presence of an external magnetic field have been extensively investigated. Many interesting experimental and theoretical results have been reported [7]. In the case of impurities in quantum dots in magnetic fields, most of the theoretical work has concentrated on donor states, using the single-band effective-mass approximation [8]. The calculations of the impurity acceptor states are much more complex than those of the corresponding donor states because of the mixing of the associated valence bands in the bulk semiconductor. Only a few papers [9, 10] dealing with calculations on the acceptor energy spectrum of highly confined systems have been reported, and they do not include the presence of a magnetic field. In this paper we investigate theoretically the influence of an external magnetic field on the energy levels of ground and excited shallow-acceptor states in quantum dots. We calculate the impurity states in the effective-mass approximation using a formalism based on a four-band model that includes the coupling of the spin to the magnetic field as well as the complicated valence-band structure of the host semiconductor. We assume that the quantum dot has the shape of a quantum disc obtained from a laterally confined $GaAs/Ga_{1-x}Al_xAs$ quantum well structure. The magnetic field is applied parallel to the disc axis. We present calculations for the energy spectrum and the binding energies of a centred acceptor impurity as a function of the dot radius and magnetic field.

2. Theory

The effective-mass Hamiltonian for the acceptor impurity in the quantum dot in the presence of a magnetic field is a 4×4 matrix operator:

$$H = H_k + H_c + H_a \tag{1}$$

where H_k is the kinetic energy of the holes, given by the Luttinger–Kohn Hamiltonian in the axial approximation [11]. It describes the dispersion of the Γ_8 valence band, and it includes the magnetic field applied in the z-direction:

$$H_k = \begin{bmatrix} a_+ & b_- & c_- & 0 \\ b_+ & a_- & 0 & c_- \\ c_+ & 0 & d_- & b_- \\ 0 & c_+ & b_+ & d_+ \end{bmatrix} \tag{2}$$

where

$$a_\pm = -\frac{\hbar^2}{2m_0}(\gamma_1 \mp 2\gamma_2)k_z^2 - \frac{\hbar^2}{4m_0}(\gamma_1 \pm \gamma_2)(k_+k_- + k_-k_+) + \kappa(2 \pm 1)\frac{1}{2}\hbar\omega_e$$

$$d_\pm = a_\pm - \hbar\omega_e\kappa(2 \pm 1)$$

$$b_\mp = \hbar^2\frac{\sqrt{3}}{4m}\gamma_3 k_z k_\mp$$

$$c_\mp = \frac{\hbar^2\sqrt{3}}{4m}(\gamma_2 + \gamma_3)k_\mp^2$$

and

$$k_\mp = -\mathrm{i}e^{\mp \mathrm{i}\phi}\left[\frac{\partial}{\partial\rho} \mp \frac{\mathrm{i}}{\rho}\frac{\partial}{\partial\phi} \pm \frac{m_0\omega_e}{2\hbar}\rho\right]$$

$$k_z = -\mathrm{i}\,\frac{\partial}{\partial z}.$$

The γ_1, γ_2, γ_3, and κ are the Luttinger parameters describing the valence band of each material composing the quantum well. The cyclotron frequency is given by $\omega_e = eB/m_0c$, where B is the applied magnetic field and m_0 is the bare-electron mass.

The geometric confinement potentials for the heavy holes and the light holes are included in the diagonal Hamiltonian H_c. They are modelled by a superposition of a quantum well potential and a lateral parabolic potential; this is

$$[H_c]_{ii} = V_0\Theta(|z| - L/2) + \frac{1}{2}m_i^*\omega_{gi}^2\rho^2. \tag{3}$$

Here $\Theta(x)$ is the Heaviside function, V_0 is the barrier height given by the valence-band discontinuity, and L is the well width. ω_{gi} is the frequency associated with the lateral geometrical confinement, and the in-plane effective masses for holes are given by $m_i^* = (\gamma_1 + \gamma_2)^{-1}m_0$, with $i = 1, 4$ for heavy holes, and $m_i^* = (\gamma_1 - \gamma_2)^{-1}m_0$, with $i = 2, 3$ for light holes.

H_a is the potential of an acceptor impurity located on the z-axis which includes the infinite set of image charges originating from the dielectric mismatch between the well and barrier materials [12]. For an impurity located on $z = z_0$ we have

$$H_a = \begin{cases} -\dfrac{(1+\beta)e^2}{\epsilon_w}\left[\dfrac{1}{\sqrt{\rho^2 + (z - z_0)^2}} + \displaystyle\sum_{q=1}^{\infty}\beta^q \frac{1}{\sqrt{\rho^2 + (z - (-1)^q z_0 - qL)^2}}\right] & z < -L/2 \\ -\dfrac{e^2}{\epsilon_w}\left[\displaystyle\sum_{q=-\infty}^{\infty}\beta^{|q|}\frac{1}{\sqrt{\rho^2 + (z - (-1)^q z_0 + qL)^2}}\right] & |z| < L/2 \\ -\dfrac{(1+\beta)e^2}{\epsilon_w}\left[\dfrac{1}{\sqrt{\rho^2 + (z - z_0)^2}} + \displaystyle\sum_{q=1}^{\infty}\beta^q \frac{1}{\sqrt{\rho^2 + (z - (-1)^q z_0 + qL)^2}}\right] & z > L/2 \end{cases} \tag{4}$$

where

$$\beta = \frac{\epsilon_w - \epsilon_b}{\epsilon_w + \epsilon_b}$$

and ϵ_w (ϵ_b) is dielectric constant in the well (barrier).

The acceptor effective Hamiltonian, H, acts on a four-component envelope function $\underline{F} = (F_1, F_2, F_3, F_4)$, and the electronic wavefunction is given approximately by

$$\psi(\vec{r}) = \sum_{\nu=1}^{4} F_\nu(\vec{r})u_0^\nu(\vec{r}) \tag{5}$$

where the $u_0^\nu(\vec{r})$ are the Γ_8 Bloch functions.

To solve the eigenvalue problem for the Hamiltonian H, we expand each component of the envelope function of the acceptor impurity, F_ν, in a complete set of basis functions which are separable in the coordinates in the plane of the disc (ρ, ϕ), and the coordinate z along the disc axis:

$$F_\nu^J(\vec{r}) = \sum_{n=1}^{n_f(\nu)} R_n^{J\nu}(\rho, \phi) f_n^\nu(z). \tag{6}$$

The z-dependent functions f_n^ν are the solutions of the one-dimensional problem for a heavy hole ($\nu = 1, 4$) or for a light hole ($\nu = 2, 3$) in a quantum well. We have neglected the contribution of the continuum states, and n runs over all of the discrete levels in the quantum well. The index J denotes the z-component of the total angular momentum of the hole, and it is a good quantum number for an impurity located on the axis of the quantum disc. For any other location of the impurity, the lateral confinement potential destroys the cylindrical symmetry, and we should expand the quantum dot envelope function in terms of functions of different angular momenta.

The radial functions in the expansion (4) are developed in a restricted set of Gaussian functions with length parameters α_k fixed *a priori* to cover the relevant physical region and ensure convergence:

$$R_n^{J\nu}(\rho, \phi) = \sum_m C_{nm}^\nu \mathrm{e}^{\mathrm{i}(J-S(\nu))\phi} \rho^{|J-S(\nu)|} \mathrm{e}^{-\alpha_m \rho^2}. \tag{7}$$

On substituting equation (7) in equation (6), the eigenvalue problem for the acceptor Hamiltonian, $H\underline{F} = E\underline{F}$, turns into a linear set of coupled equations for the coefficients of the expansion, C_{nm}^ν. The matrix elements of the kinetic energy operator H_k and the quantum dot confinement potential H_c are calculated analytically. For the calculation of the matrix elements of the impurity potential, we use the following expression:

$$\frac{1}{\sqrt{\rho^2 + \xi^2}} = \int_0^\infty \mathrm{e}^{-|\xi| y} J_0(\rho y)\, \mathrm{d}y$$

where $J_0(x)$ is the Bessel function of zero order. This procedure permits us perform the summation of the infinite series of image charges, as well as all of the integrations over the coordinates, analytically. Only the integration over the variable y, in the above equation, is calculated numerically.

3. Results

To obtain accurate acceptor energies and wavefunctions we have used a basis of 25 Gaussians, with parameters λ_j covering the range from 1 Å to 1000 Å for the in-plane coordinates. In what follows we present results for the spectrum and the binding energies of a shallow-acceptor impurity in a quantum dot in the presence of an external magnetic field. All of the numerical calculations have been performed for a quantum dot obtained by confining a $GaAs/Ga_{0.65}Al_{0.35}As$ quantum well laterally. The well width has been fixed at $L = 40$ Å. We have used the following Luttinger parameters for GaAs (AlAs): $\gamma_1 = 7.65$ (4.04), $\gamma_2 = 2.41$ (0.78), $\gamma_3 = 3.28$ (1.57), $\kappa = 1.2$ (0.12), and the dielectric constant was taken to be $\epsilon = 12.56$ (9.8). The parameters for $Ga_{1-x}Al_xAs$ are obtained by linear interpolation. We have assumed a valence-band offset of 35% and a band-gap discontinuity given by $\Delta E_g = 1.36x + 0.22x^2$.

To represent the geometrical lateral confinement we define a quantum disc radius R in terms of the expectation value of the in-plane coordinate ρ^2 in the ground state,

$$R = \sqrt{\langle \rho^2 \rangle} = \sqrt{\hbar / m_i^* \omega_{gi}}.$$

In the presence of the magnetic field there is an additional confinement induced by the field, and we can then define an effective lateral radius

$$R_{eff} = \sqrt{\hbar / m_i^* \omega_{ieff}}.$$

Here

$$\omega_{ieff} = \sqrt{\omega_{gi}^2 + \omega_{ci}^2/4}$$

is the frequency of the harmonic oscillator, the solution of the eigenvalue problem for the effective-mass hole Hamiltonian (2) in the diagonal approximation (ω_{ci} being the effective cyclotronic frequency). This effective radius can be expressed in terms of the lateral radius R, and the Landau radius

$$R_L = \sqrt{hc/eB}$$

as

$$R_{eff} = \frac{RR_L}{(R_L^4 + R^4/4)^{1/4}}.$$

The impurity binding energy is governed by the competition between two characteristic lengths, the effective Bohr radius of the acceptor in the bulk ($r_B^* \approx 67$ Å), and the effective lateral radius R_{eff}. In terms of this radius we can differentiate two different limits for the lateral confinement: the strong-confinement regime, for $R_{eff} \ll r_B^*$, in which case the binding energy should be essentially dominated by the lateral confinement showing a $1/\sqrt{(R_{eff}^2 + L^2)}$ dependence, and the weak-confinement regime, for $R_{eff} \gg r_B^*$, where it is the Coulomb interaction that plays the most important role and the binding energies should display a $1/R_{eff}^2$ dependence.

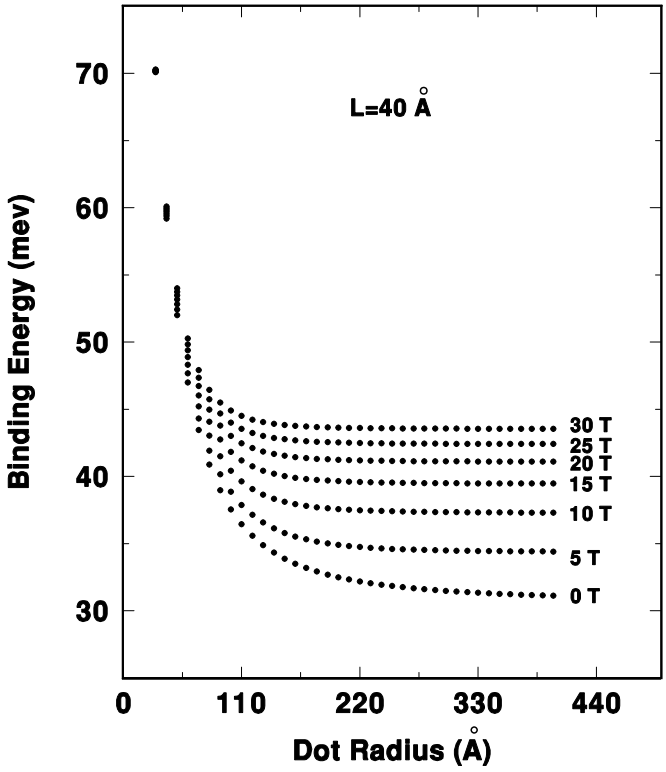

Figure 1. The dependences of the ground-state binding energies of a centred acceptor impurity in a quantum dot on the dot radius. The figure displays curves for some selected magnetic field values.

Figure 1 shows the ground-state binding energies of the centred acceptor as functions of the lateral confinement of the quantum dot. We have plotted curves for several values of the magnetic field, for quantum dot radii ranging from $R = 30$ Å to $R = 400$ Å. In the high-confinement regime we obtain the expected linear behaviour with $1/\sqrt{(R_{eff}^2 + L^2)}$ of the binding energies. In particular, in the absence of a magnetic field, a similar result was found by Xia in his work on acceptors in spherical quantum dots [10], in which he found that the binding energy decreases with $1/R_s$, where R_s is the sphere radius.

In the case of zero magnetic field and for decreasing lateral confinement, the impurity binding energy tends to the corresponding value for a 40 Å quantum well, which is approximately 30 meV for the parameters adopted. For finite values of the magnetic field the figure gives a good illustration of the competition between the geometrical confinement and the magnetic field confinement. We can see, for radii lower than 40 Å, that the binding energies are essentially dominated by the lateral geometrical confinement, giving values of the binding energy that are almost the same for all of the values of the field.

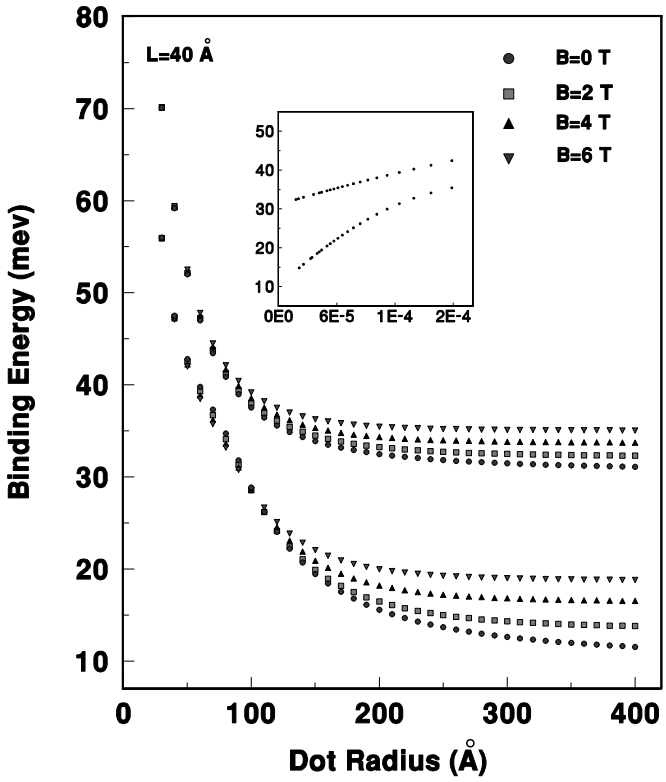

Figure 2. Binding energies of the ground state and of the first excited state, for a centred acceptor in a quantum dot, as functions of the lateral confinement. In the inset of the figure we have plotted the binding energies as functions of the inverse of the square of the effective lateral radius.

Figure 2 also shows the dependence of the impurity binding energy on the lateral confinement strength, represented by the radius of the quantum dot. In this case we have plotted the ground state and the first excited state for low values of magnetic fields. It is interesting to note that in the weak-confinement regime, for dot radii greater than 150 Å, the different set of curves, for the ground and first excited state, have the same separation in energy. This is a consequence of the linear magnetic field dependence is this regime of confinement. This feature can also be seen in the inset included in the figure, where we have plotted the binding energies as functions of $1/R_{eff}^2$. The different curves correspond to the ground and first excited state. The expected linear dependence of the binding energies on $1/R_{eff}^2$, for $R_{eff} > a_B^*$, is clearly evident. The Bohr radius for the excited state is larger than that corresponding to the ground state, and in consequence the linear behaviour arises for the larger effective radii as is illustrated in the inset. In this inset the slopes of the curves are proportional to the inverse of the effective mass of the acceptor in the plane. For the excited state the slope is three times the corresponding slope for the ground state. This is easy to understand because in the weak-confinement regime the lateral confinement energy acts as a correction to the Coulomb energy.

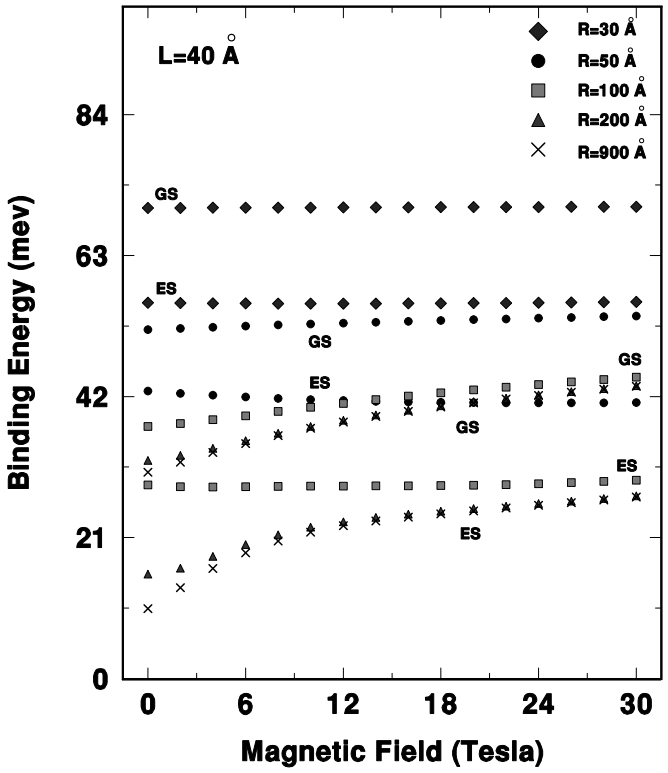

Figure 3. The magnetic field dependences of the binding energies of the ground state (GS) and the first excited state (ES), for a centred acceptor in a quantum dot. The figure displays curves for some selected dot radii.

Figure 3 shows the dependence of the acceptor binding energy on the magnetic field up to 30 T for five different quantum dot lateral radii. We have plotted in each case the ground state (GS) and the first excited state (ES). It is clearly observed that for strong lateral confinement, i.e. $R = 30$ Å and $R = 50$ Å, the acceptor binding energies are not affected by the magnetic field up to 30 T. This is because for those values of the magnetic field the lateral confinement is stronger than the confinement induced by the magnetic field (for $B = 30$ T the Landau radius is $R_L \approx 47$ Å), and the behaviour of the impurity binding energies depends fundamentally on the quantum-size confinement.

In the weak-lateral-confinement regime, for $R = 200$ Å and $R = 900$ Å, the binding energy is almost insensitive to the geometrical lateral confinement. For low magnetic fields the Coulomb interaction plays the most important role as regards the behaviour of the acceptor binding energy. When the field increases, the binding energies begin to be controlled by the magnetic confinement, displaying a $\sqrt{B}$-dependence. In the case of $R = 100$ Å there is a competition between the confining energies for a large range of magnetic field values.

In figure 4 we have plotted the acceptor energy levels as functions of the magnetic field for three different values of the lateral dot radius. We show in the same figure the calculations including (solid symbols) and neglecting (empty symbols) the effect of the mixing of heavy holes and light holes. If we do not take into account the band mixing, we know that, in the weak-confinement regime, the acceptor energies are dominated by the hole impurity Coulomb interaction, and the effect of the lateral confinement appears as a correction to the energy of an impurity in a quantum well. This term increases quadratically with the effective frequency with a curvature proportional to the inverse of the heavy-hole in-plane effective mass. On the other hand, for large dots ($R > a_0^*$) and for large values of the magnetic field ($R_L < a_0^*$), the

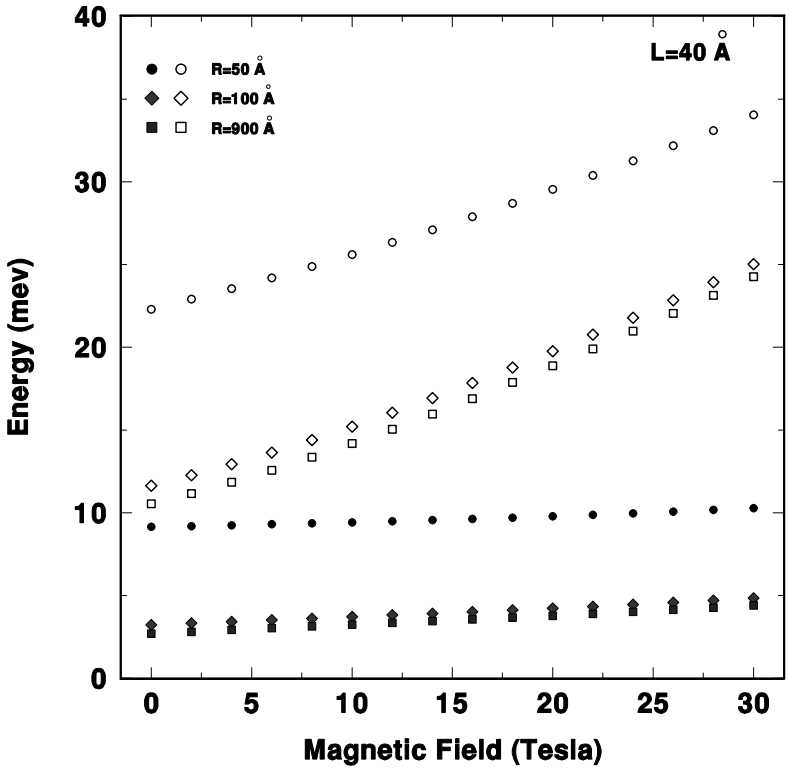

Figure 4. Acceptor energy spectra calculated including (solid symbols) and neglecting (empty symbols) the effect of the mixing of heavy and light holes. The figure displays curves for some selected dot radii.

acceptor energies have a linear dependence on the magnetic field, whose slope is given by the inverse of the heavy-hole in-plane effective mass. We see from the figure that, in both regimes, the slope decreases when the mixing is taken into account, giving clear evidence of an increase of the effective mass which is due to the presence of the light holes.

In figure 5 we compare the magnetic field dependence of the impurity binding energies calculated with (solid symbols) and without (empty symbols) the band mixing. It displays curves for some selected dot radii. The features shown by the binding energies as functions of the magnetic field can be easily understood by considering the results obtained for the ground-state impurity energy, shown in figure 4, and the corresponding analysis given in the previous section.

The quantum dot energies without impurity have a linear dependence on the effective frequency, and, therefore, in the weak-confinement regime, the binding energies present the same dependence on the effective frequency. This leads to a linear dependence of the binding energies with the magnetic field for very low lateral confinement, as we can observe for $R = 900$ Å, in the figure. In the strong-confinement limit, for large values of the magnetic field, the binding energies calculated with and without band mixing follow the same dependence with the magnetic field; this is $1/\sqrt{(R_{eff}^2 + L^2)}$. We can see that the slopes of the curves are almost the same for the two cases, showing them to be independent of the in-plane effective mass. This is an expected result if one considers the behaviour of the acceptor energies, previously analysed.

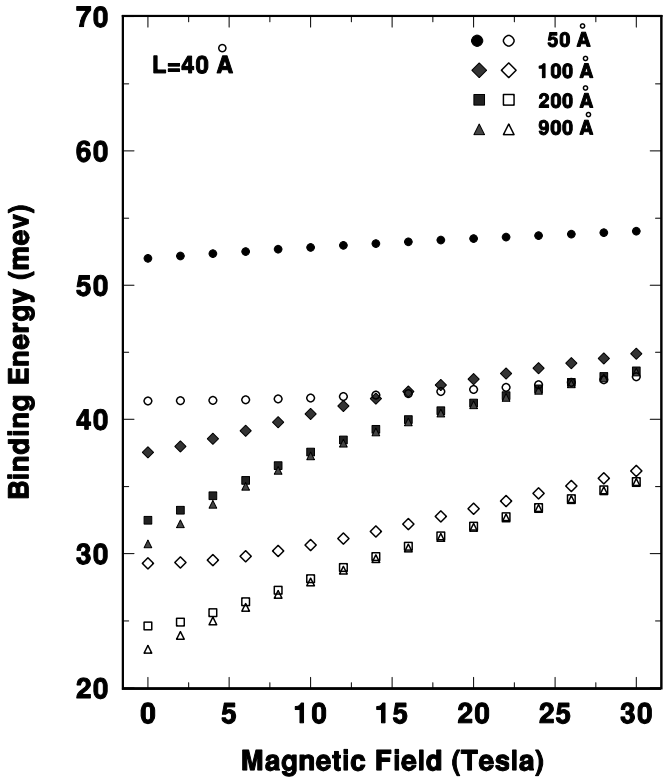

Figure 5. Impurity binding energies as functions of the magnetic field calculated including (solid symbols) and neglecting (empty symbols) the effect of the mixing of heavy and light holes. The figure displays curves for some selected dot radii.

The figure shows that for all cases the binding energy increases when the band mixing is taken into account. A simple semiclassical argument shows that the radius of an impurity depends inversely on the mass; therefore an increase in the interaction energy is again evidence of an increase of the in-plane hole effective mass.

4. Summary

To summarize, we have investigated the effect of the quantum-size confinement and the effect of an external magnetic field on the ground and the lowest-lying excited states of a centred acceptor impurity in a quantum dot. We have taken into account the mismatch of the dielectric constant and the mixing of the heavy holes and the light holes using a four-band model within the effective-mass approximation.

Our method allows computations of the energies and wavefunctions of the ground state and the excited states of an acceptor impurity in a quantum dot for a large range of confinement parameters and magnetic field strengths. It can easily be extended to apply to any position of the impurity in the dot. We have presented a complete analysis of the magnetic field dependence of the impurity binding energies in different confinement regimes. The results illustrate the competition between the magnetic field confinement and the quantum-size confinement. We have also studied the effect of the valence-band mixing on the spectrum and the binding energies of the acceptor impurity for a wide range of confinement parameters.

Although, to our knowledge, no experimental results involving acceptor impurity states in quantum dots in magnetic fields have been reported, we hope that our results might be useful in the interpretation of future experimental data.

Acknowledgments

This research was supported in part by Fondo Nacional de Ciencias, grants 1960749 and 1980225, by the Universidad de Santiago de Chile, grant 049631PD, and by the Universidad Federico Santa María, grant 971111.

References

[1] Weisbuch C, Davies J H and Long A R (ed) 1991 *Physics of Nanostructures* (Bristol: Institute of Physics Publishing)
Capasso F (ed) 1990 *Physics of Quantum Electron Devices* (Berlin: Springer)
Davies J H and Long A R (ed) 1991 *Physics of Nanostructures (Advanced Science Institute Series)*
Abstreiter G *et al* (ed) 1997 *Optical Spectroscopy of Low Dimensional Semiconductors* (Kluwer: Academic)

[2] Sotomayor-Torres C M, Wang P D, Benisty H and Weisbuch C 1992 *Low-Dimensional Electronic Systems (Springer Series in Physics vol 555)* ed G Bauer, F Kuchar and H Heinrich (Berlin: Springer) p 111
Wang P D, Song Y P, Sotomayor-Torres C M, Holland M C, Lockwood D, Hawrylak P, Palacios J J, Christianen P C M, Maan J and Perenboom J A 1994 *Superlatt. Microstruct.* **15** 23

[3] Petrof P M, Gossard A C, Logan R A and Wiegman W 1982 *Appl. Phys. Lett.* **41** 635
Cibert J, Petrof P M, Dolan G J, Pearton S J, Gossard A C and English J H 1986 *Appl. Phys. Lett.* **49** 1275
Kash K, Scherer A, Worlock J M, Craighead H G and Tamargo M C 1986 *Appl. Phys. Lett.* **49** 1043
Fukui T, Andu S, Tokura Y and Toriyama T 1991 *Appl. Phys. Lett.* **58** 2018
Lebens J A, Tsai C S, Vahala K J and Knech T F 1990 *Appl. Phys. Lett.* **56** 2642

[4] Sotomayor-Torres C M, Wang P D, Leitch W E, Benisty H and Weisbuch C 1992 *Optics of Excitons in Confined Systems* ed A D'Andrea, R Del Sole, R Girlanda and A Quattropani (Bristol: Institute of Physics Publishing)

[5] Bryant G W 1988 *Phys. Rev.* B **37** 8763
Hu Y Z, Lindberg M and Koch S W 1990 *Phys. Rev.* B **42** 1713
Le Goff S and Stébé B 1993 1989 *Phys. Rev.* B **42** 1383
Sikorski C and Merkt U 1989 *Phys. Rev. Lett.* **62** 2164
Marzin J Y, Gérard J M, Israel A, Barrier D and Bastard G 1994 *Phys. Rev. Lett.* **73** 716

[6] Bastard G 1981 *Phys. Rev.* B **24** 4714
Brown J W and Spector H N 1986 *J. Appl. Phys.* **59** 1179
Bryant G W 1984 *Phys. Rev.* B **29** 6632
Bryant G W 1985 *Phys. Rev.* B **31** 7812
Zhu J-L, Xiong J J and Gu B-L 1990 *Phys. Rev.* B **41** 6001
Einevoll G T and Chang Y C 1989 *Phys. Rev.* B **40** 9683
Zhu J L, Zhao J H and Xiong J J 1994 *Phys. Rev.* B **50** 1832
Porras-Montenegro N and Pérez-Merchancano S T 1992 *Phys. Rev.* B **46** 9780
Porras-Montenegro N, Pérez-Merchancano S T and Latgé A 1993 *J. Appl. Phys.* **74** 7652
Ribeiro F J and Latgé A 1994 *Phys. Rev.* B **50** 4913

[7] Mirlin D N and Sirenko A A 1992 *Fiz. Tverd. Tela* **34** 205 (Engl. Transl. 1992 *Sov. Phys.–Solid State* **34** 108)
Masselink W T, Chang Y-Ch and Morkoc 1985 *Phys. Rev.* B **32** 5190
Latgé A, Porras-Montenegro N and Oliveira L E 1996 *Phys. Rev.* B **53** 10 160
Ribeiro F J, Latgé A and Oliveira L E 1996 *J. Appl. Phys.* **80** 2536
Zhao Q X, Holtz P O, Pasquarello A, Monemar B, Ferreira A C, Sundaran M, Merz J L and Gossard A C 1994 *Phys. Rev.* B **49** 10 794

[8] Ferreyra J M, Bosshard P and Proetto C R 1997 *Phys. Rev.* B **55** 13 682
Li G, Branis S V and Bajaj K K 1993 *Phys. Rev.* B **47** 15 735
Ribeiro F J, Latgé A, Pacheco M and Barticevic Z 1997 *J. Appl. Phys.* **81** 12

[9] Golier V I and Polupanov A F 1993 *Fiz. Tekh. Poluprov.* **27** 1202 (Engl. Transl. 1993 *Sov. Phys.–Semicond.* **27** 663)

[10] Xia J-B 1989 *Phys. Rev.* B **40** 8500

[11] Luttinger J M 1956 *Phys. Rev.* B **102** 1030

[12] Pasquarello A, Andreani L C and Buczko R 1989 *Phys. Rev.* B **40** 5102